NATIONAL ADVISORY COMMITTEE FOR AERONAUTICS

TECHNICAL NOTE 3848

A STUDY OF SEVERAL FACTORS AFFECTING THE STABILITY CONTRIBUTED BY A HORIZONTAL TAIL AT VARIOUS VERTICAL POSITIONS ON A SWEPTBACK-WING AIRPLANE MODEL

By Gerald V. Foster and Roland F. Griner

Langley Aeronautical Laboratory
Langley Field, Va.

Washington

November 1956

NATIONAL ADVISORY COMMITTEE FOR AERONAUTICS

TECHNICAL NOTE 3848

A STUDY OF SEVERAL FACTORS AFFECTING THE STABILITY CONTRIBUTED BY A HORIZONTAL TAIL AT VARIOUS VERTICAL POSITIONS ON A SWEPTBACK-WING AIRPLANE MODEL[1]

By Gerald V. Foster and Roland F. Griner

SUMMARY

A study was made in the Langley 19-foot pressure tunnel to determine the effects of fuselage afterbody shape, split flaps, and variations in the span of the leading-edge flaps on the stability contributed by the horizontal tail to an airplane with the wing leading edge swept back 42°. Supplementary tests were made to determine some of the characteristics of the air flow in the vicinity of the tail, the wing being equipped with 0.575-span leading-edge flaps and 0.5-span split flaps. All data were obtained at a Reynolds number of 6.8×10^6.

An analysis of the air-flow surveys in the vicinity of the horizontal tail indicates that, at high angles of attack, the variation of downwash with angle of attack over the outer part of the tail span is such that the tail contribution to the pitching moment is stabilizing for the position below the extended wing-chord plane and destabilizing for the positions above the extended wing-chord plane. The air-flow surveys indicate that 20° negative dihedral would eliminate the destabilizing influence of the tail located at 16 percent of the wing semispan above the extended wing-chord plane by placing the tail in a region of favorable downwash throughout the angle-of-attack range.

The addition of split flaps decreased the stability contributed by the tail located just above the extended wing-chord plane at moderate angles of attack but increased the stability contributed by the tail at a position just below the extended wing-chord plane for angles of attack beyond 12°.

---

[1]Supersedes declassified NACA Research Memorandum L9H19 by Gerald V. Foster and Roland F. Griner, 1949.

Reducing the span of the leading-edge flaps from 0.575 wing span to 0.425 wing span improved the stability contributed by the tail located 0.16 semispan above the extended wing chord at high angles of attack but had only small effect at moderate angle of attack.

A reduction in the rate of contraction of the fuselage afterbody had a negligible effect on the stability contributed by the tail.

INTRODUCTION

The use of a sweptback wing to alleviate high-speed difficulties has posed a problem of instability near maximum lift for wings of certain combinations of aspect ratio and sweep (reference 1). Low-speed investigations of sweptback wings have indicated that longitudinal stability in the high-lift range and at stall can be obtained in some cases by the use of stall-control devices such as outboard leading-edge flaps and upper-surface fences. Consideration has been given to the effect of horizontal-tail height on the longitudinal stability of sweptback-wing airplanes in references 2, 3, and 4. Those investigations have shown that, with the horizontal tail located in the immediate vicinity of the extended wing-chord plane, relatively stable variations of pitching moment through maximum lift were obtained for all model configurations regardless of the stability of the wing-fuselage combination. It is further shown that the tail, located above the extended wing-chord plane, does not overcome the instability of the wing-fuselage combination in the high-lift range; moreover, the tail, in some cases, actually caused the pitching-moment variation of the wing-fuselage combinations, which were stable through maximum lift, to become unstable in the high-lift range. In a few instances (references 2 and 5) it has been shown that, when the vertical height of the horizontal tail was increased from a moderate height to approximately 0.5 of the wing semispan above the extended wing-chord plane, the stability of the complete model was improved.

In those cases where a decrease in the stability contributed by the horizontal tail occurred for tail positions above the extended wing-chord plane, the decrease has been attributed to the effects of unfavorable wake-induced downwash resulting from separated flow on the portion of the wing ahead of the tail. It has also been considered that the fuselage afterbody shape may produce an adverse effect on the effectiveness of the horizontal tail.

In order to furnish additional information on the contribution of the tail to longitudinal stability, an investigation has been

conducted in the Langley 19-foot pressure tunnel at a Reynolds number of 6.8×10^6 to determine the effect of fuselage afterbody shape, split flaps, and leading-edge-flap span on the stability contributed by a horizontal tail to a wing swept back 42° at the leading edge. The investigation also included a study of the flow in the vicinity of the tail. Results of this investigation are presented herein.

SYMBOLS AND COEFFICIENTS

C_L lift coefficient $\left(\frac{\text{Lift}}{qS_w}\right)$

C_m pitching-moment coefficient (moment taken about the quarter chord of the mean aerodynamic chord) $\left(\frac{\text{Moment}}{qS_w\bar{c}_w}\right)$

α angle of attack of chord plane, degrees

q dynamic pressure of the free stream, pounds per square foot $\left(\frac{\rho V^2}{2}\right)$

S area, square feet

$\bar{c}$ mean aerodynamic chord, feet $\left(\frac{2}{S}\int_0^{b/2} c^2 dy\right)$

c local chord, feet

ρ mass density of air, slugs per cubic foot

V free-stream velocity, feet per second

b span, feet

τ tail stability parameter $\left(\frac{dC_{m_t}}{d\alpha_w}\frac{1}{K}\right)$

K product of isolated tail lift-curve slope and tail volume (0.0158)

q_t/q ratio of local dynamic pressure at horizontal tail to free-stream dynamic pressure (unless otherwise noted)

ϵ local downwash angle (unless otherwise noted), degrees

σ local sidewash angle (inflow negative), degrees

$C_{m_{i_t}}$ tail-effectiveness parameter $\left(\frac{dC_m}{di_t}\right)$

i_t angle of incidence of horizontal tail measured with respect to wing-chord plane, positive when trailing edge moves down, degrees

R Reynolds number $\left(\frac{\rho V \bar{c}_w}{\mu}\right)$

M Mach number $\left(\frac{V}{\text{Velocity of sound}}\right)$

μ coefficient of viscosity

l tail length, distance in wing-chord plane from quarter-chord point of wing mean aerodynamic chord to quarter-chord point of tail mean aerodynamic chord, feet

z perpendicular distance between the extended wing-chord plane and the tail $0.25\bar{c}_t$ point

y lateral distance from plane of symmetry

Integrated air-flow surveys:

$\left(q_t/q\right)_{av}$ average q_t/q, obtained from formula

$$\frac{2}{S_t}\int_0^{b_t/2}\left(q_t/q\right)c_t db_t$$

ϵ_{av} average ϵ, obtained from formula

$$\frac{2}{\left(q_t/q\right)_{av} S_t}\int_0^{b_t/2}\epsilon\left(q_t/q\right)c_t db_t$$

Subscripts:

w	wing
t	horizontal tail
e	effective
t_{is}	isolated tail

MODEL AND APPARATUS

The model was a midwing airplane configuration having the leading edge of the wing and tail swept back 42°. The wing had an aspect ratio of 4, taper ratio of 0.625, and NACA 64_1-112 airfoil sections normal to the 0.273 chord line. The high-lift and stall-control devices employed were split flaps of $0.5\frac{b_w}{2}$ span and two spanwise leading-edge flaps, extending inboard $0.575\frac{b_w}{2}$ and $0.425\frac{b_w}{2}$ from $0.975\frac{b_w}{2}$. The horizontal tail had a plan form similar to the wing and NACA 0012-64 sections parallel to the plane of symmetry. The mounting arrangement of the tail allowed the tail to be located at several vertical positions as measured from the extended wing-chord plane. The shape of the fuselage afterbody was modified by the addition of a cylindrical cone of smaller contraction ratio than used in the investigation reported in references 2, 3, and 4. The general geometry of the model is presented in figure 1.

The six-tube survey rake of the Langley 19-foot pressure tunnel, described in reference 6, was employed to measure local dynamic pressure, sidewash, and downwash angles.

TESTS

The tests were conducted in the Langley 19-foot pressure tunnel at a dynamic pressure of approximately 75 pounds per square foot with the tunnel atmosphere compressed to about 33 pounds per square inch, absolute. For these conditions, the Reynolds number was 6.8×10^6 and the Mach number was 0.14.

Measurements of lift and pitching moment were made through a range of angle of attack from -4° to approximately 20°. The air-flow characteristics in the region of the horizontal tail were obtained (with the tail removed) at angles of attack of 3.6°, 8.5°, 13.6°, 16.8°, and 19.5°. A plane of survey, $1.93\bar{c}_w$ behind the $0.25\bar{c}_w$, was selected as a suitable plane from consideration of the fore and aft movement through the angle-of-attack range of the $0.25\bar{c}_t$ of the tail in various positions. The maximum deviation of the $0.25\bar{c}_t$ from the survey plane occurred at the high angles of attack (see fig. 2) and amounted to about 4 percent of the tail length forward and 12 percent of the tail length rearward.

RESULTS AND DISCUSSION

The force and moment data have been corrected for model-support tare and interference effects. Jet-boundary corrections have been applied to the values of angle of attack and pitching-moment coefficient. A correction for air-stream misalinement has also been applied to the values of angle of attack. The air-stream survey data have been corrected for jet-boundary effects by an angle change to the downwash and a downward displacement of the flow.

The lift and pitching-moment data are presented in nondimensional coefficient form (for only one of the two tail incidences tested) as variations with angle of attack. The effective downwash angles were determined from the tail-on and tail-off pitching-moment data. The effective values of dynamic-pressure ratio were based on a value of $C_{m_{i_t}}$ (0.0158) which was determined from the isolated tail lift-curve slope (reference 2) and the geometry of the model. It should be pointed out that this method of determining dynamic-pressure ratio takes no account of changes in tail efficiency due to the presence of the fuselage.

The combined effect of ϵ and q_t/q on the stabilizing moment contributed by the tail can be shown by considering the stability parameter τ, which is defined as follows:

$$\tau = -\left[\left(1 - \frac{\partial\epsilon}{\partial\alpha_w}\right)\frac{q_t}{q} + \alpha_t \frac{\partial(q_t/q)}{\partial\alpha_w}\right]$$

where $\alpha_t = \alpha_w \left(1 - \frac{\partial \epsilon}{\partial \alpha_w}\right) + i_t$

$$\tau = -\left\{\left(1 - \frac{\partial \epsilon}{\partial \alpha_w}\right)\left[\frac{q_t}{q} + \alpha_w \frac{\partial (q_t/q)}{\partial \alpha_w}\right] + i_t \frac{\partial (q_t/q)}{\partial \alpha_w}\right\} \qquad (1)$$

which is equivalent to

$$\tau = \frac{1}{\frac{S_t}{S_w}\frac{l}{\bar{c}_w}\left(\frac{dC_L}{d\alpha}\right)_{t_{is}}} \frac{dC_{m_t}}{d\alpha_w}$$

Inasmuch as the values of i_t were small and approximately constant for all configurations, the variations of τ with angle of attack are considered independent of stabilizer setting.

When the sign of τ is negative, it indicates that the tail is contributing stability.

Effect of Fuselage Afterbody Shape

The effect of the horizontal tail on lift and pitching-moment characteristics of the wing-fuselage combination with $0.575\frac{b_w}{2}$-span leading-edge flaps, $0.5\frac{b_w}{2}$-span split flaps, and a modified fuselage afterbody are presented in figure 3. Figure 4 shows a comparison of the variation of effective downwash angle ϵ_e, effective dynamic pressure ratio $(q_t/q)_e$, and tail stability parameter τ with angle of attack for two fuselage afterbodies of different contraction ratios. The results indicate that, with the tail in the highest position, reducing the contraction ratio of the fuselage afterbody had a negligible effect on τ which resulted from negligible effects of both $(q_t/q)_e$ and ϵ_e. When the tail was located close to the wing-chord plane extended, reducing the afterbody rate of contraction increased $(q_t/q)_e$ and $d\epsilon_e/d\alpha_w$, which are opposite effects, as

indicated in equation (1) and tend to counteract each other as shown by very little change in τ.

Effect of Leading-Edge-Flap Span

Previous data have shown that when leading-edge flaps are used to improve the longitudinal stability of sweptback wings near maximum lift, flow separation has been found to occur initially on the inboard sections of the wings. In the case of the present wing with $0.575\frac{b_w}{2}$-span leading-edge flaps, flow separation occurred in the region of the inboard end of the leading-edge flaps (reference 7). Inasmuch as the stability contributed by the horizontal tail is dependent on the air flow in which the tail operates, an attempt was made to shift the initial separation on the wing by shortening the $0.575\frac{b_w}{2}$-span leading-edge flaps $0.15\frac{b_w}{2}$ from the inboard end and consequently altering the flow behind the wing.

The lift and pitching-moment data obtained with and without split flaps are presented in figures 5(a) and 5(b). The variation of ϵ_θ, $(q_t/q)_\theta$, and τ with angle of attack are presented in figure 6. The effect of reducing the span of the leading-edge flaps on the stability contributed by the tail can be seen by comparing the stability-parameter curves for the configuration with split flaps (figs. 4 and 6). It can be seen that the stabilizing effect of the tail was not appreciably changed throughout the angle-of-attack range except for the tail height of $0.162\frac{b_w}{2}$. For that tail height in conjunction with wing configurations with either the short-span or the long-span leading-edge flaps, there is a decrease, through moderate angles of attack, in the stability contributed by the tail, which is indicated by the positive increase in the value of τ. At high angles of attack, the long-span leading-edge flaps cause the tail to have no stabilizing effect ($\tau = 0$), whereas with the short-span flaps, the tail was highly stabilizing ($\tau = -0.65$). These effects are indicated by the pitching-moment variation obtained for the complete configurations (figs. 3 and 5(a)).

Effect of Split Flaps

The effect of the split flaps in conjunction with $0.425\frac{b_w}{2}$-span leading-edge flaps on the tail stability parameter (fig. 6) appears most pronounced for the tail positions close to the wing-chord plane extended. The split flaps appear to produce a flow, at moderate angles of attack, that causes a decrease in the stability contributed by the tail located $0.162b_w/2$ above the extended wing-chord plane, while at high angles of attack the initial degree of stability is regained. The results without split flaps indicate that the tail located $0.162b_w/2$ above the extended wing-chord plane contributes stability through the angle-of-attack range with only a gradual decrease at the moderate and high angles of attack. For the case where the tail is located $-0.061b_w/2$ below the extended wing-chord plane, the results without split flaps indicate that the tail contributed a constant amount of stability through the angle-of-attack range; the addition of split flaps caused increases in stability contributed by the tail for angles of attack beyond 12°.

Air-Flow Characteristics at the Tail

In order to provide further insight as to the stabilizing effect contributed by the tail with the wing equipped with $0.575\frac{b_w}{2}$-span leading-edge flaps and split flaps, results of air-flow survey in the vicinity of the tail are presented in figure 7 as contours of dynamic-pressure ratio, downwash angle, and sidewash angle. A cross plot of downwash angle at several tail spanwise stations with angle of attack is presented in figure 8 for various tail arrangements. Average values of ϵ and q_t/q have been determined for 0.417 and $0.162b_w/2$ tail heights where survey data were complete. Determination of these values was based on the assumption that the measured values of ϵ and q_t/q were the actual local conditions affecting the tail. It may be seen in table I that the average values of ϵ and q_t/q are in fair agreement with the effective values for the corresponding tail positions.

It may be seen from contours of dynamic-pressure ratio that the low tail is located in or below the wake throughout the angle-of-attack range. At an angle of attack of 16.8°, the results indicate a broadening of the wake and an upward shift of the wake center outboard of station $0.20b_w/2$. These wake changes cause a decrease in downwash

(reference 8) in the region of the low tail so that, at high angles of attack, the outboard portion of the tail is operating in a region where the rate of change of downwash with angle of attack, as affected by the span-load distribution and induced wake effects, is highly stabilizing. (See fig. 8.)

Upon considering the tail location $0.162b_w/2$ above the extended wing-chord plane, it may be seen that the outboard part of the tail enters the field of high downwash at a moderate angle of attack and remains in it through the high angle-of-attack range. Throughout the angle-of-attack range, the position of the tail relative to the wake is such that the induced-wake effects would increase the downwash at the tail. Figure 8 indicates that in the moderate angle-of-attack range the variation of downwash angle with angle of attack is adverse at both the tip and root regions of the tail. At high angles of attack, the unfavorable downwash which occurs in the tip region affects a greater portion of the span inboard; however, the stabilizing variation of downwash angle with angle of attack at the root appears to be highly influential on the over-all effect of the tail. (See fig. 4.)

At high angles of attack, the decrease in stability contributed by the tail in the high position is shown to result from an undesirable variation of downwash with angle of attack on the outer part of the tail. This adverse downwash is the result of the combined effects of the spanwise distribution of load and wake-induced downwash.

It is of interest to note that the adverse effect which occurs with the tail just above the fuselage might possibly be eliminated by incorporating negative dihedral in the tail. The variation of downwash with angle of attack at several spanwise stations of a tail with approximately -20° dihedral and an equivalent projected span (fig. 8) indicates highly stabilizing values of $\frac{\partial \epsilon}{\partial \alpha_w}$ at high angles of attack. A tail with dihedral is affected not only by the downwash component of the flow but also by the sidewash component. Consideration of the sidewash indicated that the effect was negligible up to approximately 14° angle of attack, beyond which the positive sidewash in the region of the tip would cause an increase in the angle of attack of the tail. In order to show more clearly the effects of negative tail dihedral on the pitch characteristics, the pitching moments have been calculated from the survey data for the tail located $0.162b_w/2$ above the extended wing-chord plane with and without dihedral. (See fig. 9.) Comparison of the calculated and experimental curves for the tail without dihedral (figs. 3 and 9) indicates that

the accuracy of the calculated curves is sufficient to show the stability trends. The results of calculations indicate that negative dihedral eliminates the instability at high angles of attack which was noted for the tail without dihedral.

A comparison of air-flow-survey results presented herein and in reference 6 indicates that the major effects of the fuselage occurred inboard of station $0.20b_w/2$. These effects appeared as an upward shift of the wake center and an alteration of the downwash pattern. In general, however, they appear to have only small effects on the influence of the tail.

It should be pointed out that the tail, at a given position, contributes essentially the same variation in stability for the unflapped-wing configurations as for the flapped-wing configurations; however, the reason for the decrease in stability contributed by the tail to the unflapped-wing configurations at high angles of attack is somewhat different than the reason previously discussed for the flapped-wing configurations. The unflapped wing stalls at the tip and causes an increase in loading on the inboard sections of the wing and a resultant increase in downwash.

CONCLUDING REMARKS

The results of a study of several factors affecting the stability contributed by a horizontal tail to a model airplane with 42° sweptback wing equipped with leading- and trailing-edge flaps are as follows:

1. An analysis of the air-flow surveys in the vicinity of the horizontal tail indicates that, at high angles of attack, the variation of downwash with angle of attack over the outer sections of the tail span is such that the tail contribution to the pitching moment is stabilizing for the position below the extended wing-chord plane and destabilizing for the positions above the extended wing-chord plane. The air-flow surveys indicate that 20° negative dihedral would eliminate the destabilizing influence of the tail located at 0.162 wing semispan above the extended wing-chord plane by placing the tail in a region of favorable downwash throughout the angle-of-attack range.

2. The addition of split flaps decreased the stability contributed by the tail located just above the extended wing-chord plane at moderate angles of attack but increased the stability contributed by the tail at a position just below the extended wing-chord plane for angles of attack beyond 12°.

3. Reducing the span of the 0.575-span leading-edge flaps to 0.425 improved the stability contributed by the tail located 0.16 semispan above the extended wing-chord plane at high angles of attack but had only small effect at moderate angles of attack.

4. A reduction in the rate of contraction of the fuselage afterbody had a negligible effect on the stability contributed by the tail.

Langley Aeronautical Laboratory,
National Advisory Committee for Aeronautics,
Langley Field, Va., August 22, 1949.

REFERENCES

1. Shortal, Joseph A., and Maggin, Bernard: Effect of Sweepback and Aspect Ratio on Longitudinal Stability Characteristics of Wings at Low Speeds. NACA TN 1093, 1946.

2. Spooner, Stanley H., and Martina, Albert P.: Longitudinal Stability Characteristics of a 42° Sweptback Wing and Tail Combination at a Reynolds Number of 6.8×10^6. NACA RM L8E12, 1948.

3. Foster, Gerald V., and Fitzpatrick, James E.: Longitudinal-Stability Investigation of High-Lift and Stall-Control Devices on a 52° Sweptback Wing With and Without Fuselage and Horizontal Tail at a Reynolds Number of 6.8×10^6. NACA RM L8I08, 1948.

4. Woods, Robert L., and Spooner, Stanley H.: Effects of High-Lift and Stall-Control Devices, Fuselage, and Horizontal Tail on a Wing Swept Back 42° at the Leading Edge and Having Symmetrical Circular-Arc Airfoil Sections at a Reynolds Number of 6.9×10^6. NACA RM L9B11, 1949.

5. Schuldenfrei, Marvin, Comisarow, Paul, and Goodson, Kenneth W.: Stability and Control Characteristics of a Complete Airplane Model Having a Wing With Quarter-Chord Line Swept Back 40°, Aspect Ratio 2.50, and Taper Ratio 0.42. NACA TN 2482, 1951. (Supersedes NACA RM L7B25.)

6. Furlong, G. Chester, and Bollech, Thomas V.: Effect of Ground Interference on the Aerodynamic and Flow Characteristics of a 42° Sweptback Wing at Reynolds Numbers up to 6.8×10^6. NACA Rep. 1218, 1955. (Supersedes NACA RM L8G22 and NACA TN 2487.)

7. Graham, Robert R., and Conner, D. William: Investigation of High-Lift and Stall-Control Devices on an NACA 64-Series 42° Sweptback Wing With and Without Fuselage. NACA RM L7G09, 1947.

8. Silverstein, Abe, Katzoff, S., and Bullivant, W. Kenneth: Downwash and Wake Behind Plain and Flapped Airfoils. NACA Rep. 651, 1939.

TABLE I

EFFECTIVE AND AVERAGE VALUES OF DYNAMIC-PRESSURE RATIO AND DOWNWASH ANGLE AT THE TAIL OF A 42° SWEPTBACK WING-FUSELAGE COMBINATION, LEADING- AND TRAILING-EDGE FLAPS DEFLECTED

Tail height $b_w/2$		α				
		3.6°	8.5°	13.5°	16.8°	19.5°
0.417	$(q_t/q)_{av}$	1.00	1.00	1.01	1.00	1.02
	$(q_t/q)_e$	1.02	0.98	0.98	1.02	1.02
	ϵ_{av}	3.9°	6.4°	8.7°	10.5°	13.9°
	ϵ_e	4.9°	6.8°	9.0°	10.9°	14.0°
0.162	$(q_t/q)_{av}$	1.00	1.02	0.97	0.94	0.89
	$(q_t/q)_e$	0.97	0.92	0.94	0.87	0.80
	ϵ_{av}	5.8°	8.0°	11.4°	14.7°	15.6°
	ϵ_e	6.1°	8.2°	10.6°	12.9°	16.3°

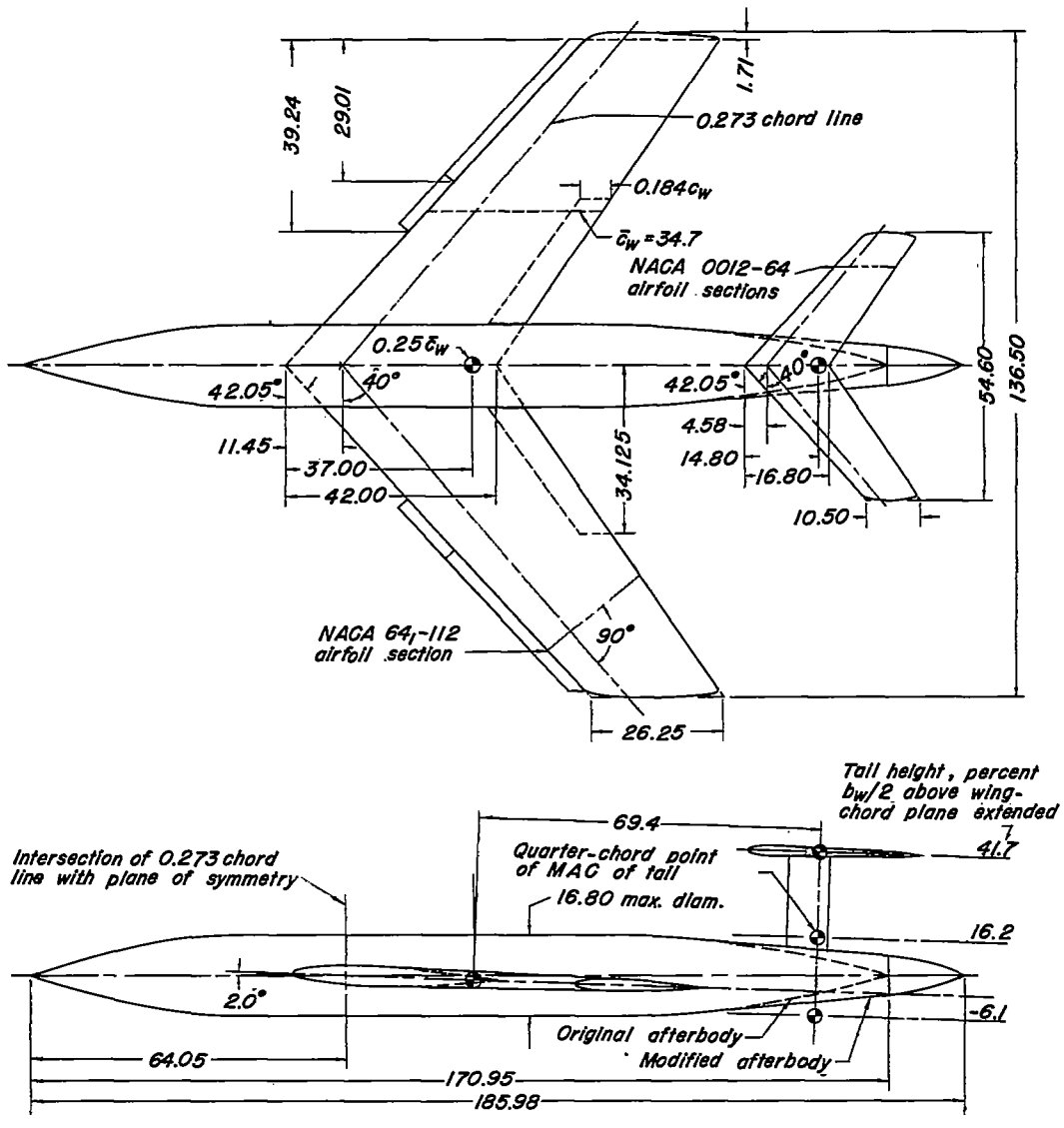

FUSELAGE ORDINATES					
Distance behind fuselage nose	Original fuselage diameter	Distance behind fuselage nose	Original fuselage diameter	Distance behind fuselage nose	Modified fuselage diameter
0	0.20	112.00	16.80	132.00	14.90
18.00	9.84	122.00	16.32	170.95	8.00
22.05	11.80	132.00	14.90	174.11	7.66
27.39	13.80	142.00	12.52	177.23	6.68
34.56	15.60	151.20	9.46	180.28	5.04
42.35	16.60	162.00	4.78	183.23	2.78
48.00	16.80	170.95	0	185.98	0

Figure 1.— Geometry of model with leading-edge flaps and split flaps. Aspect ratio, 4.01; taper ratio, 0.625. All dimensions are in inches.

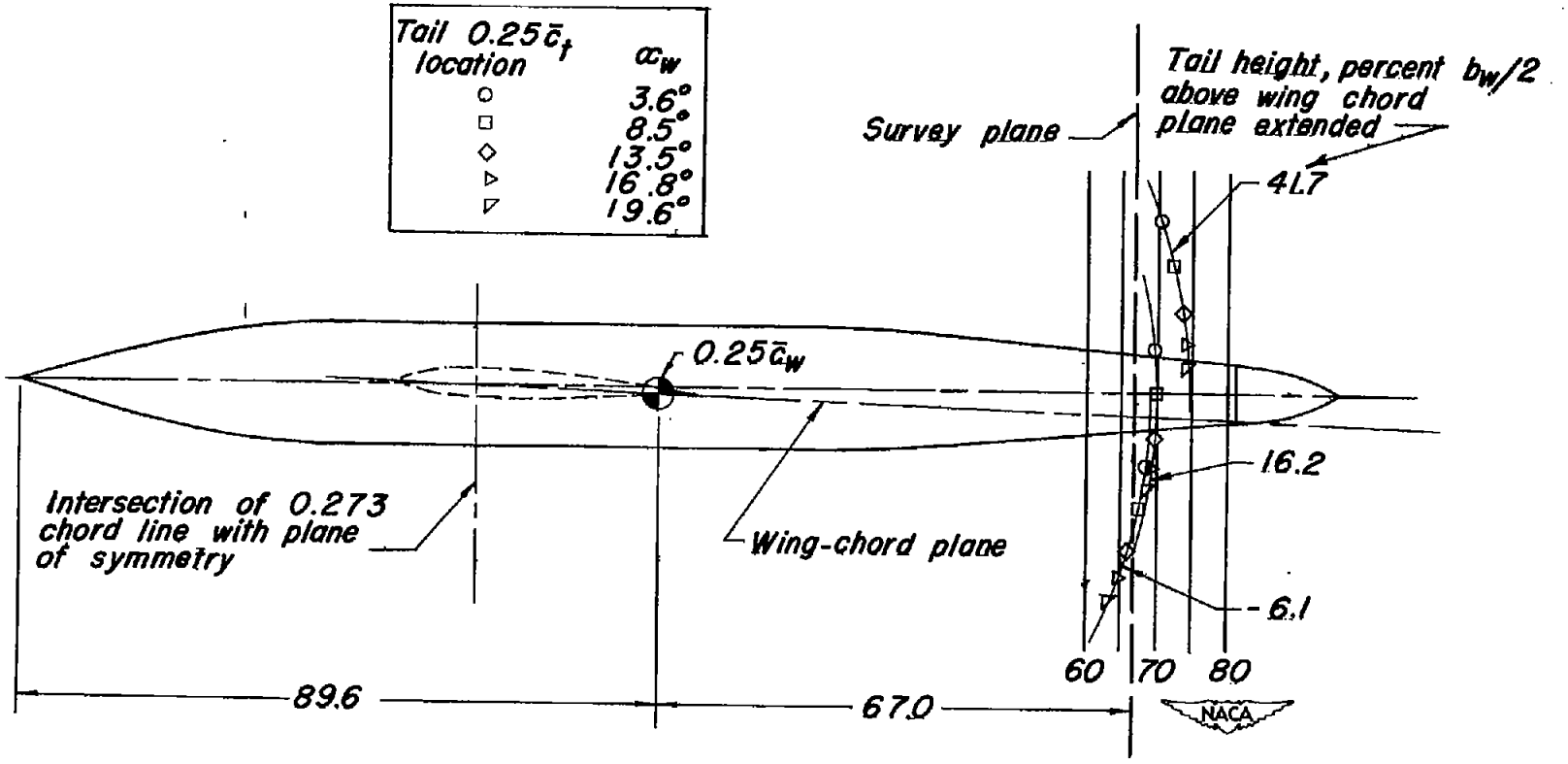

Figure 2.– Variation of 0.25$\bar{c}_t$ of the tail with respect to the survey plane for the angle-of-attack range. All dimensions are in inches.

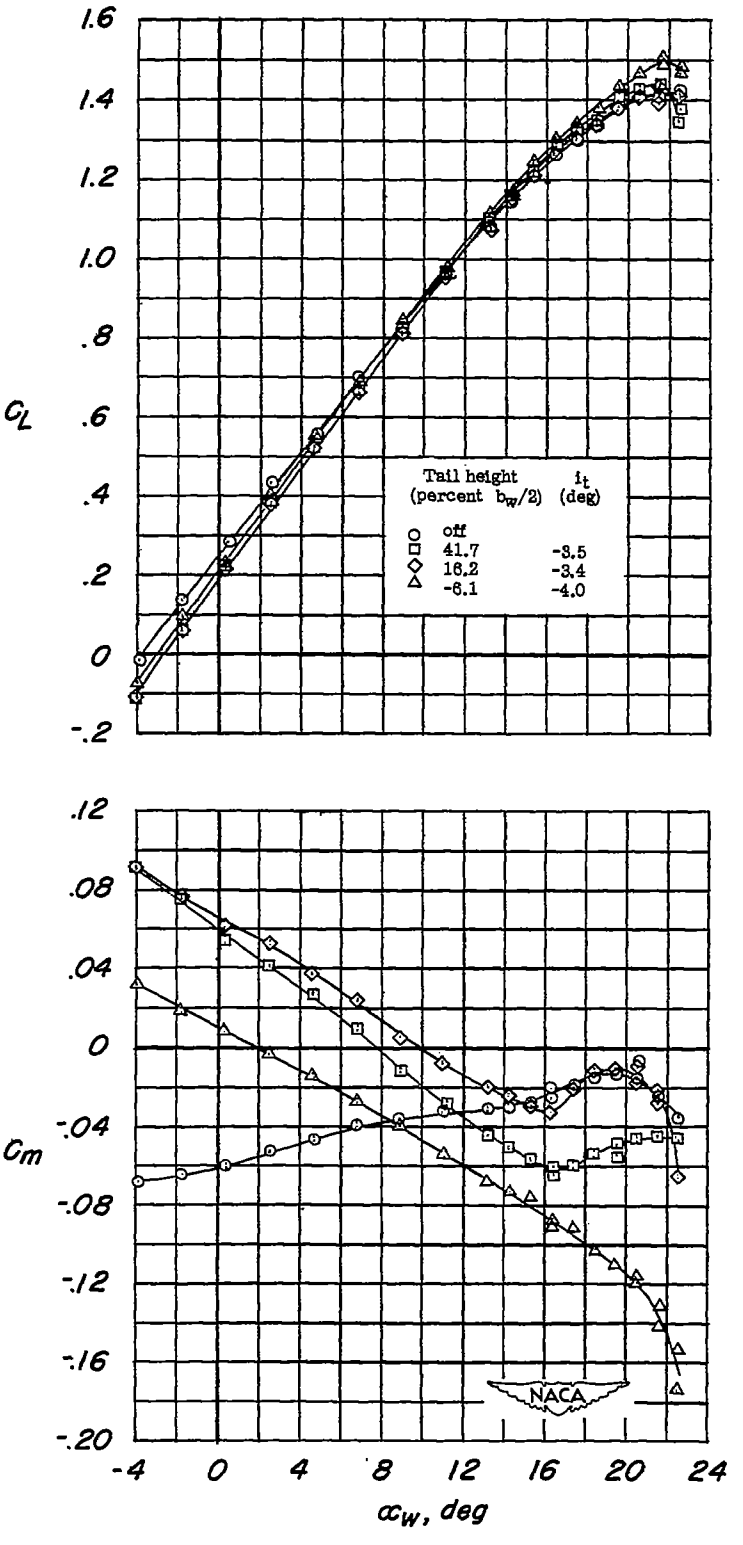

Figure 3.- Aerodynamic characteristics of a 42° sweptback-wing fuselage with horizontal tail; $0.575b_w/2$ leading-edge flaps and $0.5b_w/2$ split flaps; modified afterbody; $R = 6.8 \times 10^6$; $M = 0.14$.

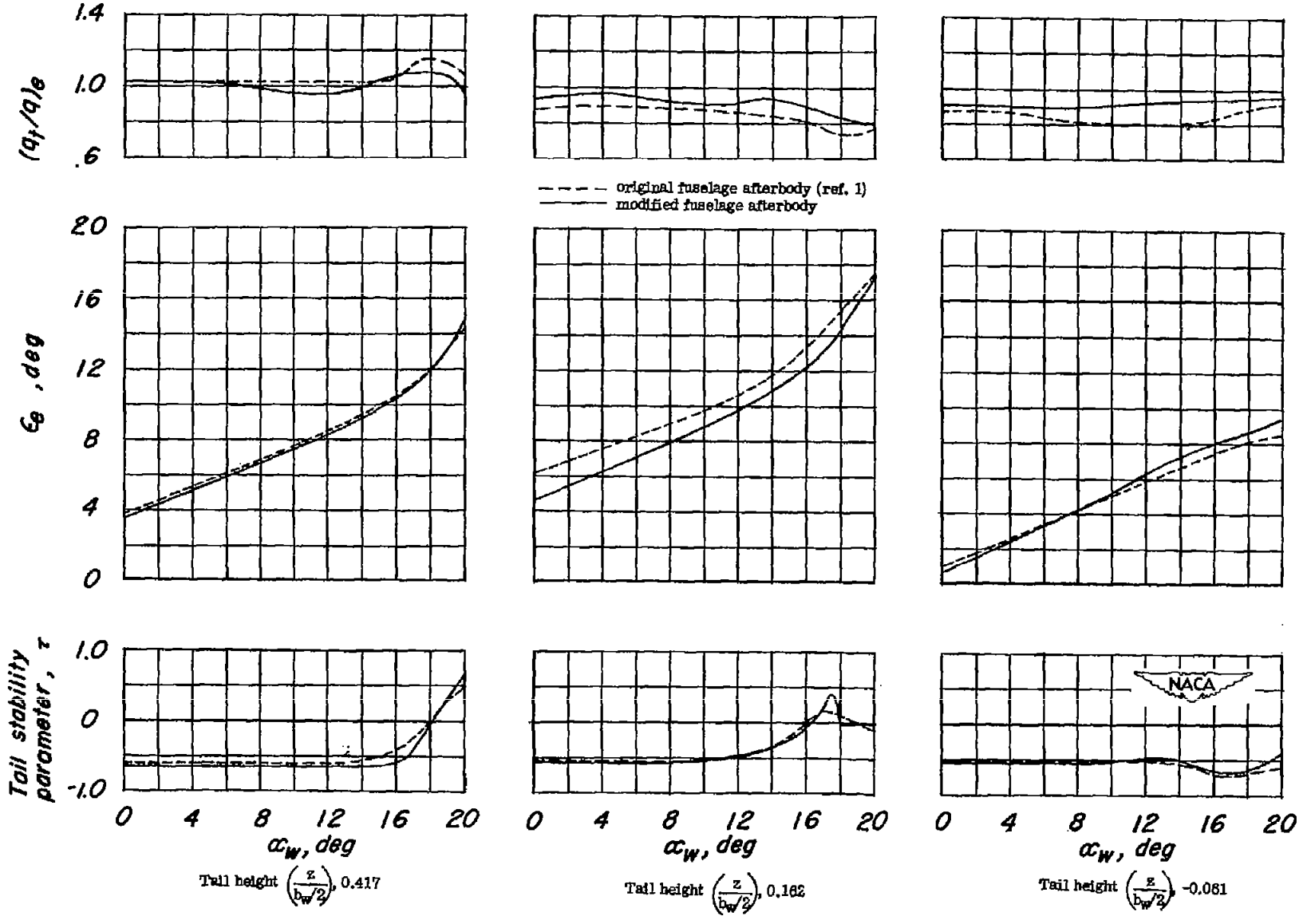

Figure 4.– Effect of fuselage afterbody shape on ϵ_ϵ, $(q_t/q)_\epsilon$, and τ for several tail heights; $0.575b_w/2$ leading-edge flaps and split flaps.

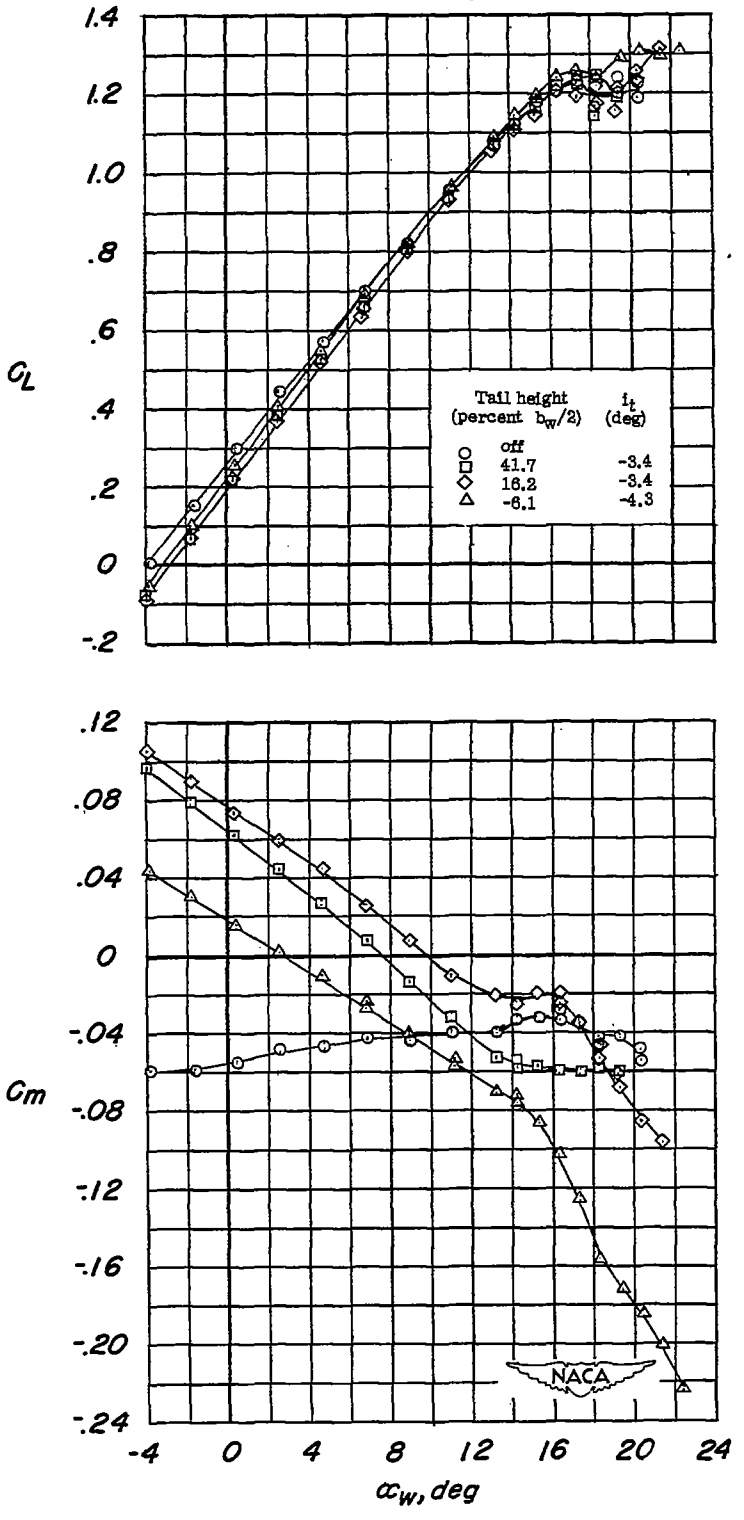

(a) Split flaps on.

Figure 5.- Aerodynamic characteristics of a 42° sweptback wing fuselage with horizontal tail; $0.425b_w/2$ leading-edge flaps; modified afterbody; $R = 6.8 \times 10^6$; $M = 0.14$.

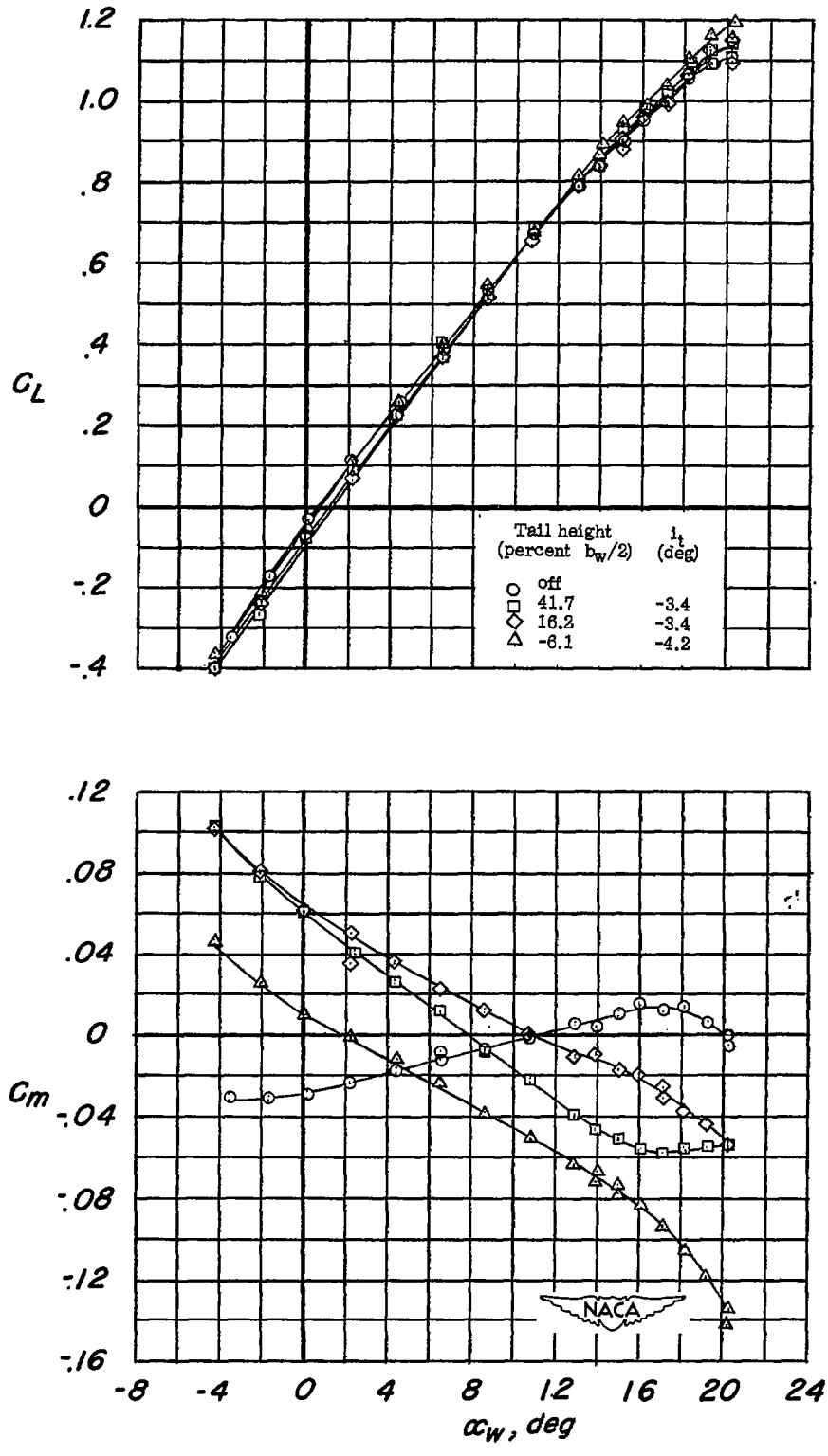

(b) Split flaps off.

Figure 5.– Concluded.

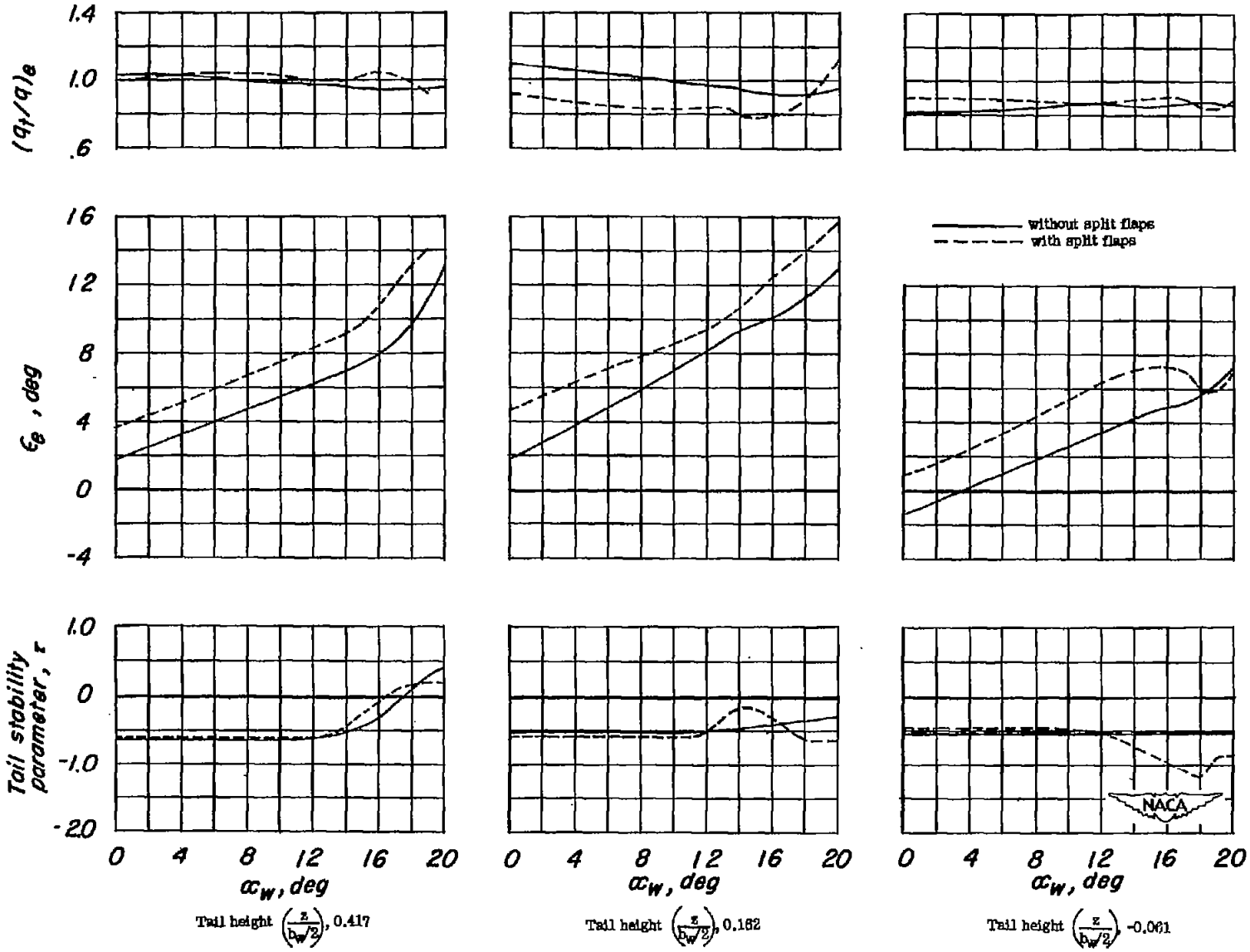

Figure 6.– Effect of split flaps on ϵ_e, $(q_t/q)_e$, and τ for several tail heights; $0.425b_w/2$ leading-edge flaps; modified afterbody.

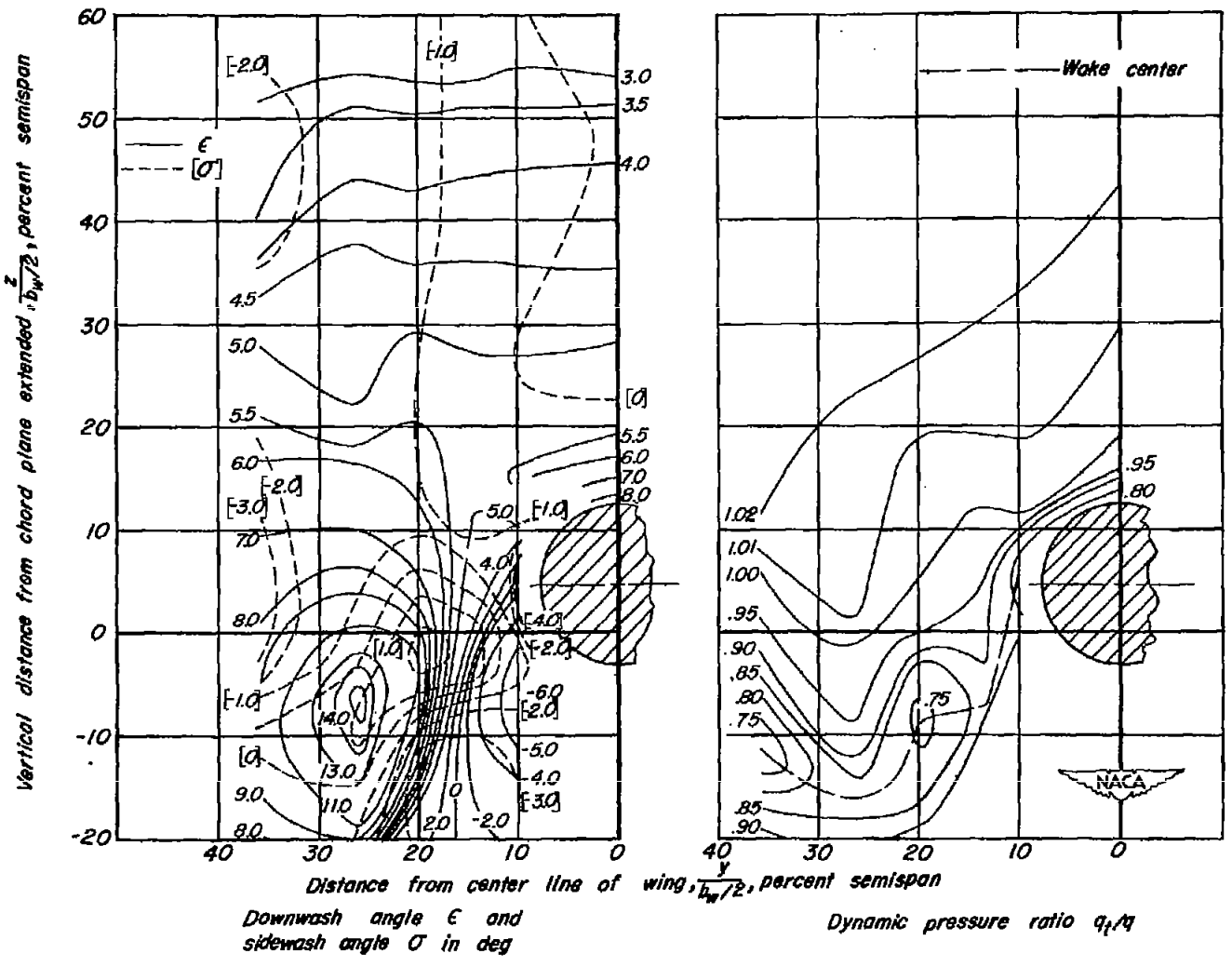

(a) $\alpha_w = 3.6°$.

Figure 7.– Contours of downwash, sidewash, and dynamic–pressure ratio behind a 42° sweptback wing fuselage in the region of a horizontal tail; $0.575b_w/2$ leading-edge flaps and split flaps; modified afterbody; $R = 6.8 \times 10^6$; $M = 0.14$.

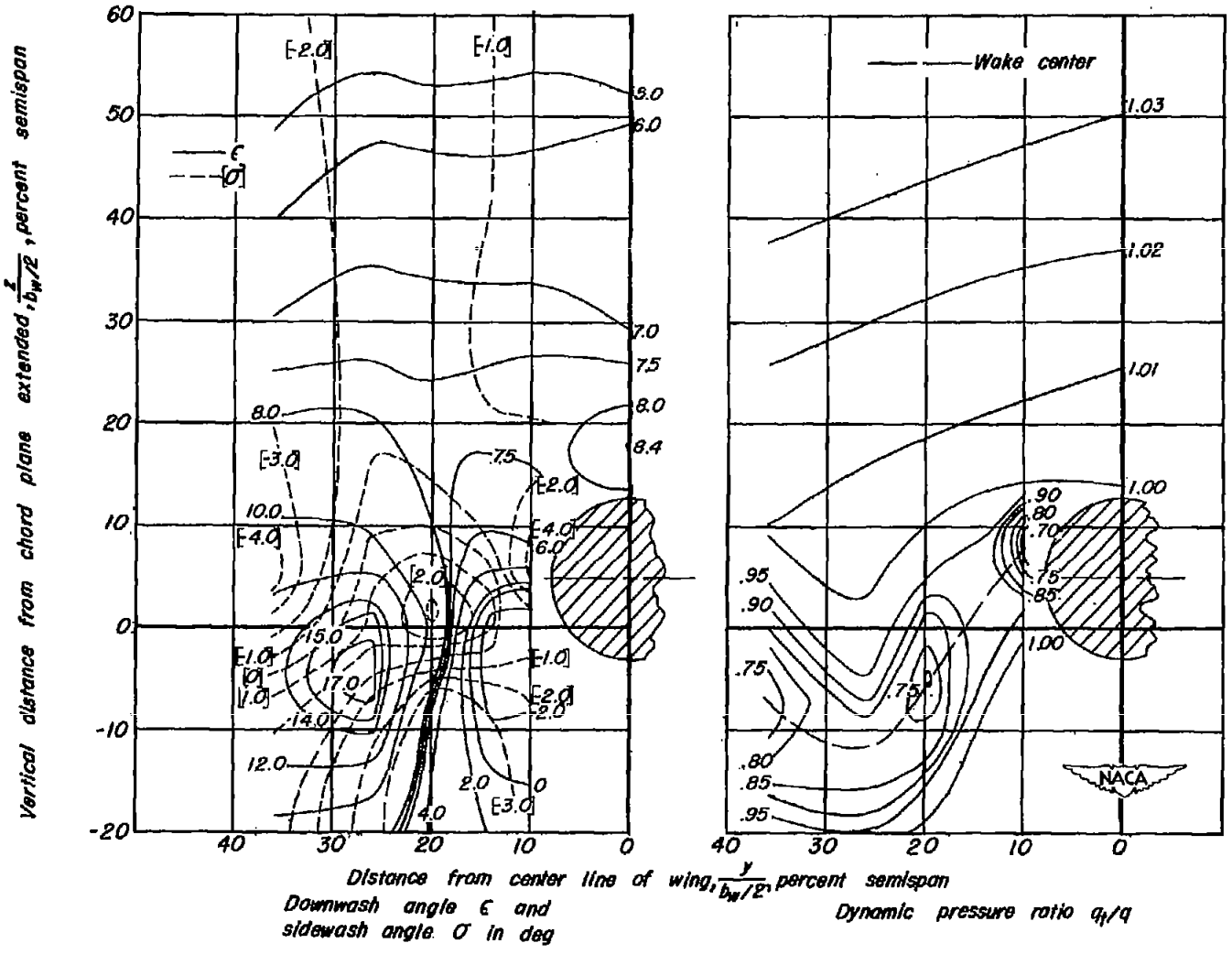

(b) $\alpha_w = 8.5^\circ$.

Figure 7.– Continued.

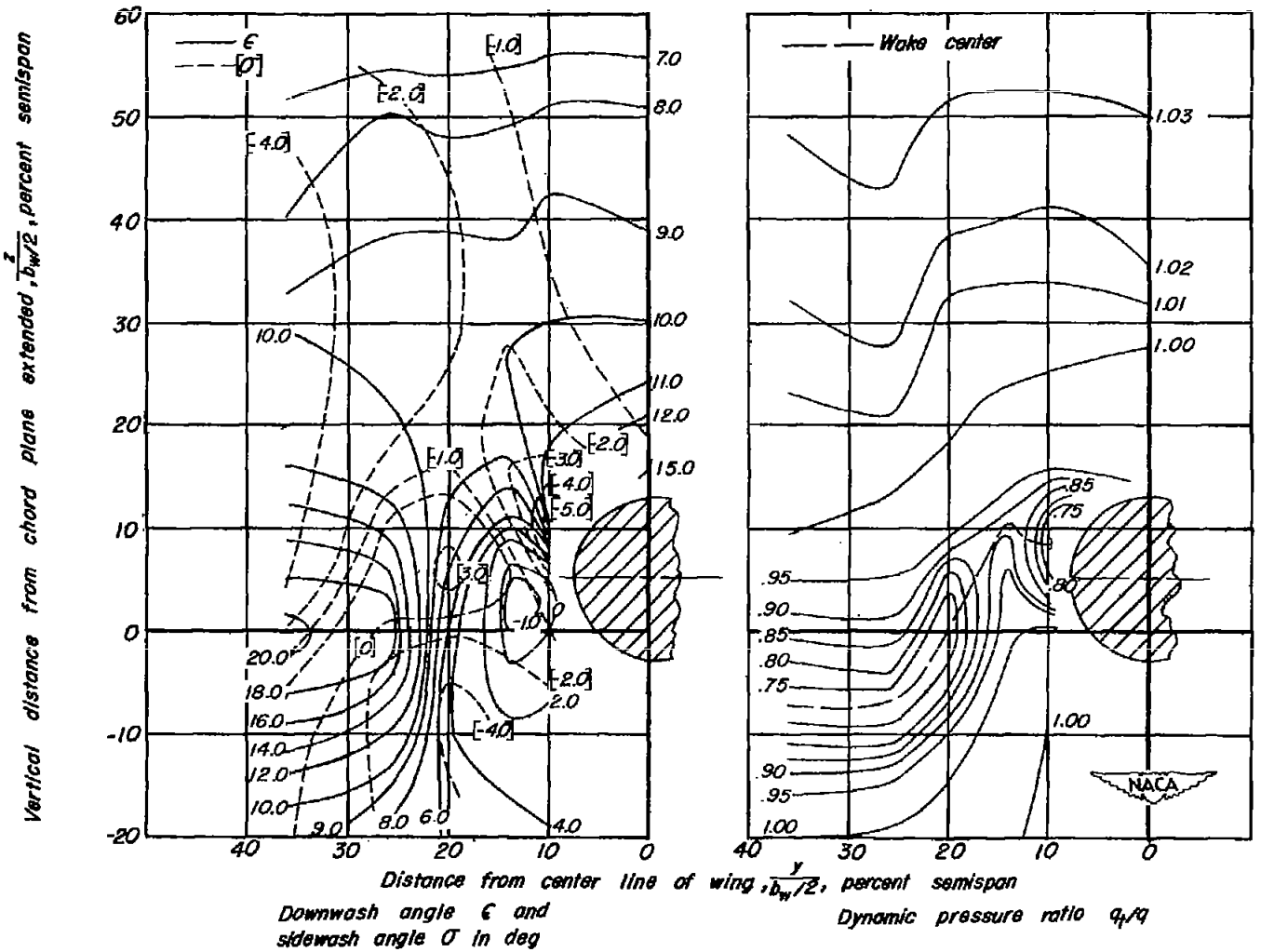

(c) $\alpha_w = 13.5°$.

Figure 7.– Continued.

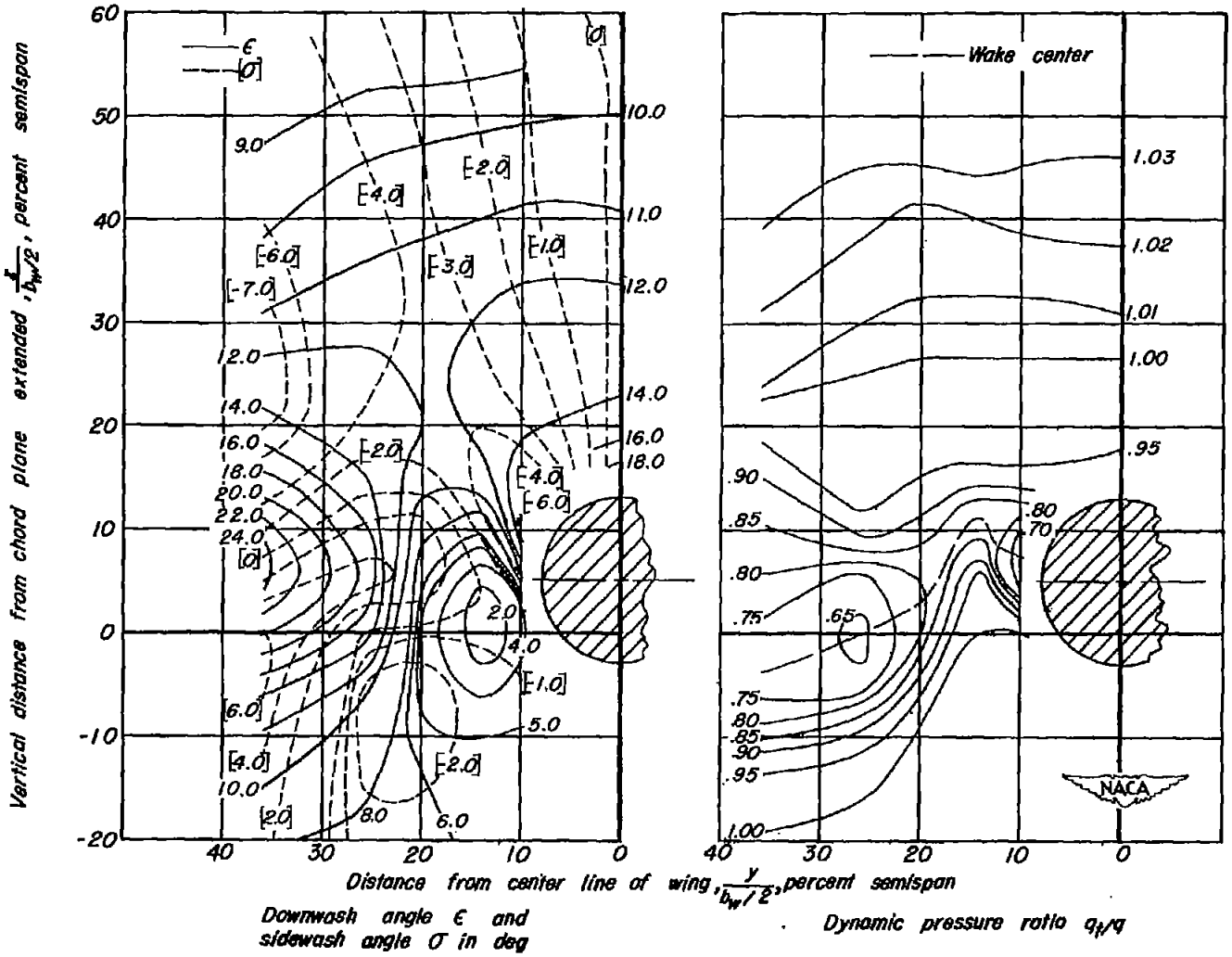

(d) $\alpha_w = 16.8°$.

Figure 7.– Continued.

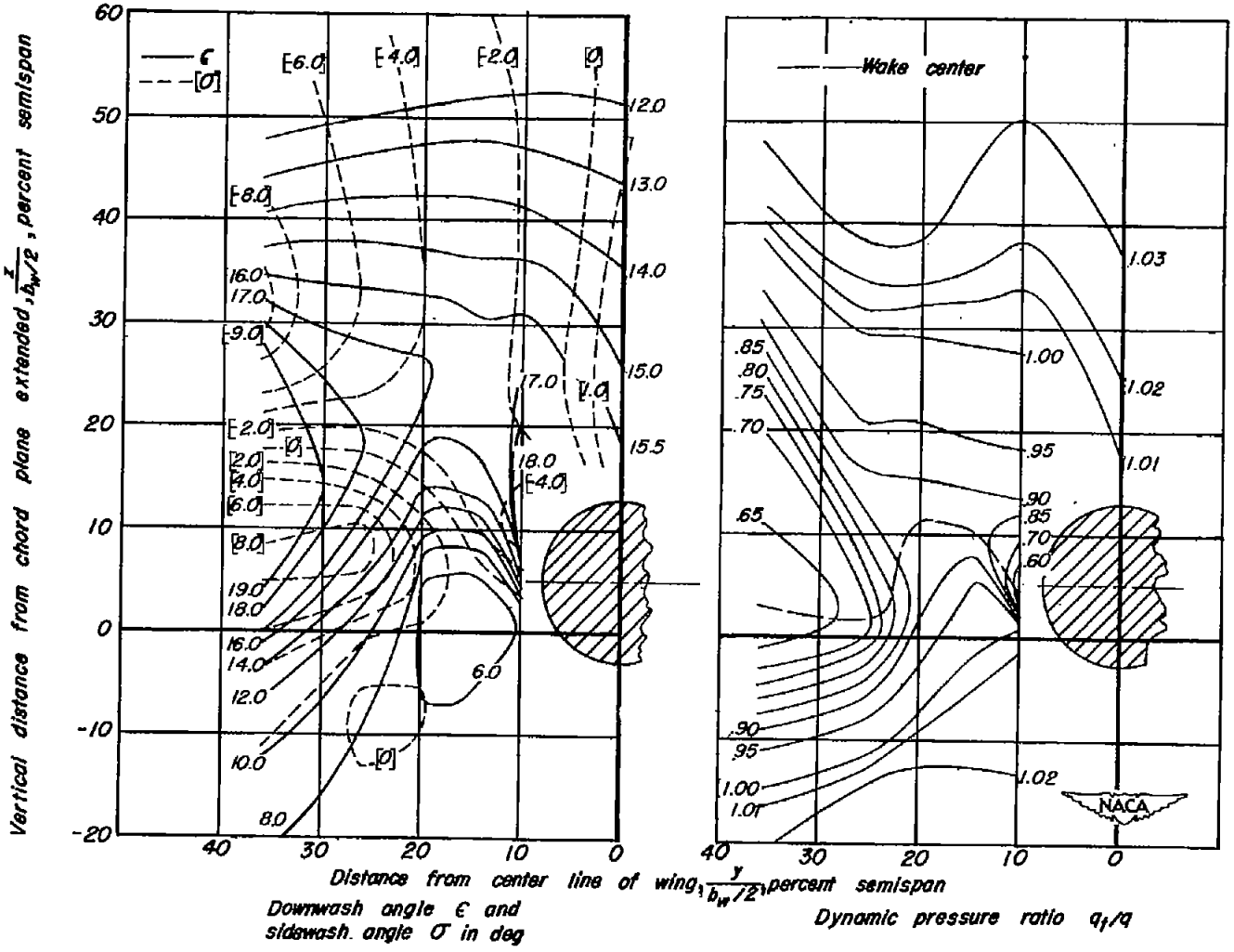

(e) $\alpha_w = 19.5^\circ$.

Figure 7.– Concluded.

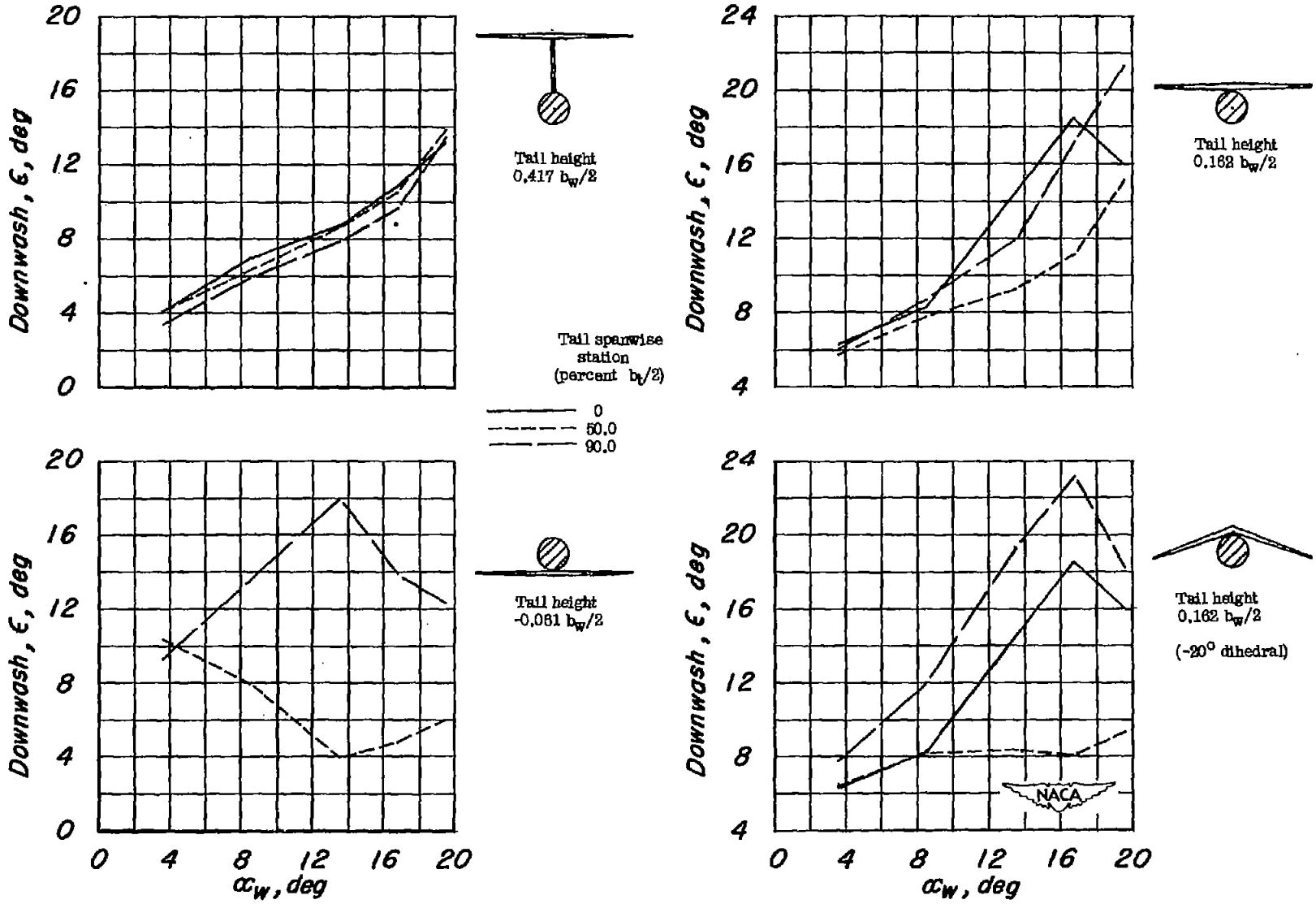

Figure 8.– Variation of downwash angle of several spanwise stations of various tail arrangements; $0.575b_w/2$ leading-edge flaps and split flaps.

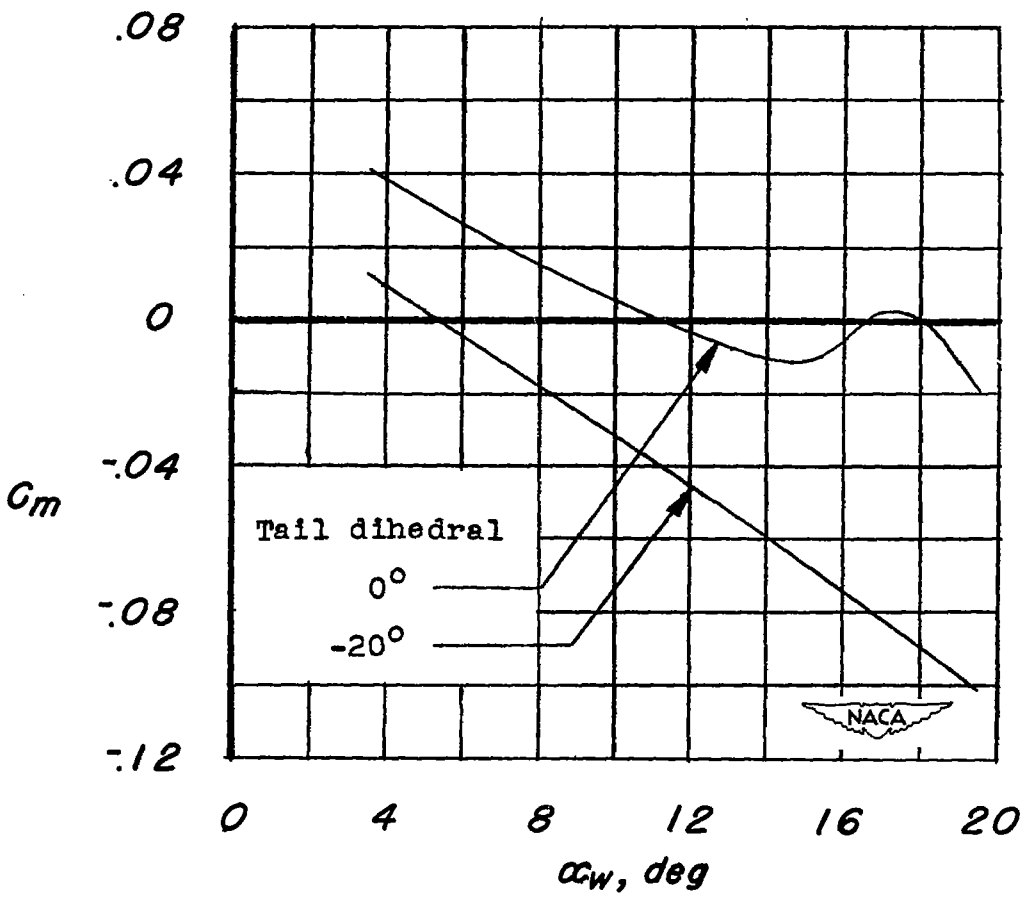

Figure 9.– Variation of calculated pitching-moment coefficient with angle of attack; tail height $0.162b_w/2$.

NACA - Langley Field, Va.